Conformational Properties of the β(400–436) and β(400–445) C-Terminal Peptides of Porcine Brain Tubulin†

Jennifer Reed,‡ William E. Hull,§ Herwig Ponstingl,‖ and Richard H. Himes*,⊥

Department of Pathochemistry, Central Spectroscopy Department, and Project Molecular Biology of Mitosis, German Cancer Research Center, Heidelberg, Federal Republic of Germany, and Department of Biochemistry, University of Kansas, Lawrence, Kansas 66045-2106

Received June 10, 1992; Revised Manuscript Received September 10, 1992

ABSTRACT: Two peptides from the C-terminal region of the major β-tubulin isotype (400–436 and 400–445) that include the critical areas for interaction with MAP2 and tau were examined to determine their conformations in aqueous solution. Despite a high theoretical potential for α-helix formation, CD spectroscopy showed that these peptides consisted primarily of random coil with some reverse turn. This was unaffected by the presence of counterions to the negatively charged side chains (Ca^{2+}, Mg^{2+}), but did change when the side-chain charges were neutralized by lowering the pH; under these conditions, the α-helix content of the longer peptide rose to 25% and the C-terminal truncated peptide to 15%. The peptides also adopt α-helical structure in the presence of trifluoroethanol, the truncated peptide again attaining a lower maximum percentage. The β(400–445) peptide was also studied by 1-D and 2-D NMR techniques. The results indicate that at pH 5.6 or 7 in an aqueous solution the peptide is extremely flexible and lacks regular secondary structure, consistent with the CD results. Both peptides inhibited microtubule-associated protein-stimulated tubulin assembly, with the longer peptide being about 4 times as inhibitory as the smaller peptide. Neither was inhibitory in the absence of microtubule-associated proteins, indicating that interaction with this species was necessary for inhibition. The greater activity of the longer peptide could be due to the extra negative charges in this peptide and/or the greater tendency of this peptide to form an α-helical structure under the appropriate conditions.

The C-terminal regions of the α- and β-subunits of tubulin are known to be important in the control of the polymerization of the protein into microtubules. A number of studies have demonstrated that these regions contain binding sites for the microtubule-associated proteins (MAPs)[1] MAP2 and tau (Serrano et al., 1984a, 1985; Littauer et al., 1986; Maccioni et al., 1988; Vera et al., 1988; Cross et al., 1991) and for Ca^{2+} (Serrano et al., 1986; Vera et al., 1989). Specific regions within the C-termini appear to be the major sites of interaction with MAPs. For example, α-tubulin residues (430–441) and β-tubulin residues (422–434) are known to be involved in the binding of MAP2 and tau (Maccioni et al., 1988; Rivas et al., 1988; Vera et al., 1989). Littauer et al. (1986) concluded that residues 434–440 of β-tubulin are critical for the interaction of MAP2 and tau.

The α- and β-chains of the ubiquitous brain isotypes contain 451 and 445 amino acid residues, respectively, the last 40 of which are composed of approximately 40% Glu and Asp (Little & Seehaus, 1988). This gives rise to highly negatively charged C-terminal regions of the molecule. It is likely that some of these negative charges are involved in interactions with MAPs. Removal of these regions of the two chains with subtilisin (Serrano et al., 1984b, 1988; Sackett et al., 1985; Bhattacharyya et al., 1985; White et al., 1987; Kanazawa & Timasheff, 1989) or modification of the carboxyl groups to neutral amides (Mejillano & Himes, 1991) increases the polymerization efficiency of tubulin and decreases its interaction with MAPs. The susceptibility of the C-terminal tails to limited proteolysis by subtilisin and the availability of epitopes in these regions to antibodies, when tubulin is in the polymerized form (Breitling & Little, 1986), suggest that these regions of the polypeptides are exposed to the solvent.

This study was undertaken to determine the conformational properties in aqueous solution of two peptides from the major β-tubulin isotype in porcine brain (400–436 and 400–445), the latter representing the last 46 amino acids in the β-chain. Previous studies have examined the structure of much shorter peptides from the α C-terminal (Sugiura et al., 1987; Otter & Kotovych, 1988) and β C-terminal (Otter et al., 1991) regions, and most of these studies were done in organic solvents or in mixed organic/aqueous solvents.

EXPERIMENTAL PROCEDURES

Materials. The β(400–436) peptide was obtained from Applied Biosystems as a crude mixture and was purified by RP-HPLC on an analytical Zorbax C8 column using a 50 mM NH_4HCO_3 (pH 7.0)/60% CH_3CN in 20 mM NH_4HCO_3 gradient. The major fraction contained the β(400–436) peptide. After lyophilization, the peptide was dissolved in 0.1 M NH_4HCO_3, and the sequence of the peptide was confirmed using an Applied Biosystems 475A protein sequencer. The N^{α}-acetyl-β(400–445) peptide in pure form was purchased from Cambridge Research Biochemicals and dissolved in 10 mM sodium phosphate, pH 7.4.

† This work was supported by National Institutes of Health Grant GM 36953 and a Fullbright travel grant.

* Address correspondence to this author.

‡ Department of Pathochemistry, German Cancer Research Center.

§ Central Spectroscopy Department, German Cancer Research Center.

‖ Project Molecular Biology of Mitosis, German Cancer Research Center.

⊥ Department of Biochemistry, University of Kansas.

[1] Abbreviations: Pipes, piperazine-*N*,*N*′-bis(2-ethanesulfonic acid); EGTA, ethylene glycol bis(β-aminoethyl ether)-*N*,*N*,*N*′,*N*′-tetraacetic acid; GTP, guanosine 5′-triphosphate; DMSO, dimethyl sulfoxide; RP-HPLC, reversed-phase high-pressure liquid chromatography; CD, circular dichroism; TFE, trifluoroethanol; MAPs, microtubule-associated proteins; PBS, phosphate-buffered saline.

0006-2960/92/0431-11888$03.00/0

The concentrations of the peptide solutions were calculated from the absorbance at 275 nm. Each peptide contains two Tyr and two Phe residues, the latter contributing little to the 275-nm absorbance. Trp is not present in the peptides. The UV absorption spectrum was identical to that expected for Tyr with a maximum of 275–276 nm. A molar extinction coefficient of 2800 M^{-1} cm^{-1} (the molar extinction coefficient of Tyr is 1400 M^{-1} cm^{-1}) (Sober, 1968) was used to calculate the concentrations.

Pipes and EGTA were purchased from Sigma Chemical Co. GTP was obtained from Boehringer Mannheim. [^{3}H]-GTP at a specific activity of 12.8 Ci/mmol was a product of Dupont.

Preparation of Tubulin and MAPs. Tubulin free of MAPs was prepared as previously described (Algaier & Himes, 1988). The procedure involves the isolation of microtubule protein from bovine brain by three cycles of assembly/disassembly (Shelanski et al., 1973), the third cycle being done in 0.4 M Pipes/10% DMSO (Himes et al., 1977), followed by chromatography on a phosphocellulose (Whatman P11)–Biogel P-10 piggyback column. Purified tubulin was drop-frozen in liquid nitrogen and stored at −80 °C.

A crude MAP preparation was prepared from bovine brain by the procedure described by Drubin and Kirschner (1986) with the exception that the protein solution was concentrated by ultrafiltration instead of by ammonium sulfate precipitation.

Assembly Assay. A microassembly assay was developed because of the high cost of the peptides. Typical spectrophotometric assays utilize 0.5-mL volumes. The assay was based on the filter assay described by Maccioni and Seeds (1978) and modified for use in steady-state dynamic studies of MAP-free microtubules (Wilson et al., 1982; Stewart et al., 1990). A 1 mg/mL tubulin solution in PEM buffer (0.1 M Pipes, pH 6.9, 1 mM EGTA, and 1 mM $MgSO_4$) containing 0.5 mM [^{3}H]GTP (40 cpm/pmol) and other components (MAPs, peptides, 10% DMSO, e.g.) was aliquoted as 20-μL volumes into 1.5-mL Eppendorf centrifuge tubes which were incubated at 37 °C for 10 min, after which 1 mL of a microtubule stabilizing solution (0.75% glutaraldehyde, 50% sucrose, and 5 mM ATP in PEM) at 37 °C was added. The solution was filtered immediately through Whatman GF/F 2.4-cm glass fiber filters. The filters were washed immediately with two 3-mL volumes of PEM containing 30% glycerol (v/v) and 0.75% glutaraldehyde at 37 °C. The filtering and washing procedure for each sample was completed within 20 s. Filters were transferred to scintillation vials, and 0.5 mL of 0.1 M NaOH was added. After 30 min, 10 mL of Packard Scint A XF scintillation fluid was added and the samples were counted. Corrections were made for control samples lacking MAPs or DMSO. In calculation of the amount of assembly, a factor of 0.7 was used for the amount of [^{3}H]GTP which exchanged into the tubulin dimer.

Circular Dichroism Spectra. Circular dichroism (CD) spectra of the peptides were measured using a Jasco J-500 automatic-recording spectral polarimeter coupled to a J-DPY digital data processor. The instrument was calibrated using a 0.05% β-androsterone solution in dioxane. The slit width was held automatically at 1.0 nm throughout the spectral range.

Far-UV CD spectra were taken from 190 to 240 nm using a sensitivity setting of 2 deg/cm, a scan speed of 5 nm/min, a time constant of 2.0 s, and a wavelength expansion of 5 nm/cm. Samples were measured at a concentration of 65–84 μg/mL in 10 mM phosphate buffer, pH 7.4, with modifications as given in the figure legends. A 1.0-mm quartz cuvette was used throughout. The spectra presented are the products of 4-fold signal-averaged spectra digitally recorded in millidegrees with an identically signal-averaged solvent base line subtracted; these were converted to θ_{mr} (mean residue ellipticity) for curve-fitting and secondary structure analysis. Curves were fitted as the linear sum of the CD spectra of model peptides in purely α-helix, β-sheet, random or extended coil, and reverse-turn conformations. For the first three structure types, curves from the literature employing various homo- and heteropolymers with different side chains were combined, weighted according to the frequency of occurrence of the side chain concerned in proteins in general. Reverse-turn model curves were taken from Crisma et al. (1984).

^{1}H-NMR Spectroscopy. ^{1}H-NMR spectra of the N^{α}-acetyl-β(400–445) synthetic peptide (MW = 5257) were obtained at 500 MHz using a Bruker AM-500 FT-NMR spectrometer. For initial studies, a sample of 13 mg of peptide in 0.5 mL of PBS/D_2O buffer was prepared by first adding the lyophilized peptide to 0.35 mL of buffer at pH 7. The pH dropped to ca. 4.5, preventing complete dissolution of the peptide. Small aliquots of NaOD solution and phosphate/D_2O buffer were added to neutralize the sample, and the peptide was dissolved completely. Final concentrations were approximately 5 mM peptide, 18 mM sodium phosphate, and 60 mM NaCl, pH 6.98. For measurements in H_2O, this sample was lyophilized, and after addition of H_2O, the pH was adjusted to 5.6 to slow peptide NH exchange. Chemical shifts are reported relative to internal trimethylsilyl [2,2,3,3-$^2H_4$]-propionate (TSP).

The following NMR experiments were carried out in D_2O at pH 6.98 (meter reading), using conventional presaturation of the residual water signal: 1-D spectra at 10, 20, and 25 °C; phase-sensitive 2-D COSY-DQF (Rance et al., 1983); 2-D RELAY with three coherence-transfer steps (Wagner, 1983); 2-D J-resolved and 2-D ROESY (rotating-frame Overhauser effect) (Bax & Davis, 1985) using the pulsed spin-lock method (Kessler et al., 1987; Reed et al., 1988) with an effective B_1 field of ca. 2.5 kHz and a mixing time of 0.3 s [also see Hull (1987) for a description of pulse sequences]. In H_2O at pH 5.6, NH proton exchange was sufficiently slow, and water presaturation was used for all experiments. Both 1-D and 2-D measurements (COSY, NOESY with a mixing time of 0.4 s, and ROESY with a mixing time of 0.3 s) were performed at 30 °C.

For the 1-D spectra shown in the figures, water suppression was performed with a presaturation time of 3 s and with the lowest possible power for CW irradiation. A 32K FID with 512 transients was accumulated with a spectral width of 4065 Hz (D_2O) or 5208 Hz (H_2O). The repetition times and flip angles were 7 s, 60° (D_2O) and 6 s, 90° (H_2O). Mild Lorentz–Gauss resolution enhancement was applied (Bruker GM routine, LB = −1.4 Hz, GB = 0.3). For a high-resolution COSY-DQF experiment (D_2O), a spectral width of 2358 Hz (aliphatic region) and a t_2 time domain of 4K points were used. A total of 16 transients for each of 1024 t_1 values were acquired with TPPI phase cycling and a repetition time of ca. 3 s (17-h experiment). Sine-bell window functions shifted $\pi/4$ in t_2 and $\pi/6$ in t_1 and zero-filling were applied before Fourier transformation to give an 8-Mword data matrix. COSY and NOESY in H_2O were performed as magnitude-mode experiments with a spectral width of 4098 Hz for 2K t_2 points; 32 or 64 (NOESY) transients for each of 512 t_1 values were acquired with a repetition time of 2.3 s. Sine-bell window functions and zero-filling were used for the Fourier transformation. The phase-sensitive ROESY experiment in

FIGURE 1: Amino acid sequence of the tubulin β(400–445) peptide and secondary structure potential. P_α is plotted as the average helix probability across a five-residue window, where $P_\alpha > 1.03$ is considered favorable to helix formation. Regions of especially high probability are shown as shaded boxes. Potential β-reverse turns are indicated by arrowed brackets.

H_2O was performed with a spectral width of 4098 Hz and a t_2 domain of 2K. The spin-lock was applied as ca. 30° pulses with a duty cycle of 10%. A total of 32 transients for each of 800 t_1 values were acquired.

RESULTS

NMR Spectroscopy. The amino acid sequence of the N^α-Ac-β-tubulin(400–445) peptide is shown in Figure 1. There is an N-terminal Gly bearing the *N*-acetyl group (denoted here as G^1) and an unblocked C-terminal Ala (A^{46}). The peptide is extremely rich in negatively charged side chains (5 Asp, 14 Glu), and the application of folding algorithms (Chou & Fasman, 1978) reveals a high potential for helix formation along virtually the entire length of the peptide, with up to 4 reverse turns (β-bends) also having high probabilities.

In D_2O solution, the following aliphatic proton spin systems should be present (Wüthrich 1986): 4 AB: 4 G; 13 ABX: 5 D, 2 N, 2 S, 2 F, 2 Y; 4 A_3X: 4 A; 2 A_3MX: 2 T; 21 AB(MN)X: 3 M, 14 E, 4 Q; 1 A_3B_3MX: 1 V; 1 A_3B_3(PQ)-RX: 1 L; 4 A_3: 1 NAc, 3 M methyls; for a total of 208 nonexchangeable aliphatic protons. In addition, 2 AA'BB'-(Y) and 2 AA'BB'C(F) spin systems will contribute 18 aromatic protons. Figure 2 presents the aliphatic proton regions of the one-dimensional 500-MHz spectrum of the peptide in PBS/D_2O buffer at neutral pH. The high resolution and uniformity in signal line widths is striking and more typical of the appearance of spectra for small peptides of 5–10 residues than for spectra of small globular proteins. The purity of the sample was extremely good, and careful integration of the spectrum, together with spin system information present in the COSY-DQF and RELAY spectra, allowed us to accurately account for all 208 aliphatic protons (labeling in Figure 2) and all 18 aromatic protons (see Figure 4). All exchangeable protons had been lost to the solvent by the time of the first NMR measurement ca. 1 h after sample preparation. Except for the multitude of overlapping Glu and Gln signals, all 2-D cross-peak patterns could be assigned to specific types of amino acid residues. The G^1 α-protons gave a pseudosinglet (near-equivalence), indicating free rotation at the N-terminal end. The A^{46} methyl group (1.355 ppm) appeared upfield of the other three Ala methyls (1.41–1.43 ppm) due to the proximity of the negatively charged C-terminal carboxyl group. The natural line width for A^{46} (ca. 1.5 Hz) was about half that observed for the other Ala residues (ca. 3 Hz), again indicating somewhat higher mobility at the C-terminal end. There were only minor changes in chemical shifts with temperature, and at 20 °C, there was no overlap of the water signal with the Hα region.

The relatively narrow, uniform line widths (2–3 Hz for Hα) across the entire spectrum suggest that the peptide must have significant segmental mobility and little or no stable secondary or tertiary structure. Furthermore, the spin systems for the various types of amino acid residues fall neatly into groups with chemical shifts close to those measured for model tetrapeptides (Wüthrich, 1986). Figure 3 illustrates this for the $\alpha\beta1$, $\alpha\beta2$ proton COSY cross-peaks for 11 ABX systems. For example, the five Asp spin systems show <0.1 ppm spread in chemical shifts. The vicinal coupling constants fall in the range $J_{\alpha\beta1}$ = 5.5–6 Hz and $J_{\alpha\beta2}$ = 8–9 Hz for all 11 systems and are indicative of significant conformational averaging about the χ^1 angle. Similarly, the two Ser residues give nearly equivalent signal patterns (α = 4.43 ppm, $\beta1$ = 3.88 ppm, $\beta2$ = 3.83 ppm), three Gly residues have chemical shifts within the range 3.88–4.08 ppm, three Ala are very similar, the three Met ζCH_3 are only partially resolved (one at 2.104 ppm, two at 2.099 ppm), and the two Phe side chains as well as the two Tyr are virtually indistinguishable (see Figure 4). The two Thr α-protons are nearly identical (4.30 and 4.31 ppm), but for one residue, Hβ and γCH_3 are shifted upfield by 0.08 and 0.03 ppm, respectively, which suggests that this is probably the F-T^{10}-E triad with stronger shielding effects compared to the A-T^{30}-A triad. Finally, a ROESY experiment in D_2O (data not shown) gave all the expected intraresidue Overhauser effects for the side chains, but there were no clearly recognizable interresidue effects.

Figure 4 presents the aromatic proton and NH regions from the 1-D spectrum of the peptide in H_2O buffer at pH 5.6, chosen to slow down base-catalyzed NH exchange without significant protonation of the side-chain carboxyl groups. For the aliphatic protons, there were only very minor changes in chemical shifts relative to those at pH 7 (Figure 2). Integration of the spectrum showed that at least 40 of the 46 possible peptide NH protons were visible, despite some transfer of saturation from the suppressed water signal. All 12 of the nonequivalent side-chain amide protons (2 Asn, 4 Gln) could also be accounted for (assigned by virtue of COSY and NOESY cross-peaks between geminal amide protons). Remarkably uniform peptide NH line widths were observed at 30 °C, indicating uniformly slow exchange. Figure 5 presents the NH–Hα correlation region from a low-resolution COSY experiment. At least 40 cross-peaks are present, and some assignments could be made by inspection. Cross-peaks for Hα = 4.6–4.7 ppm are weak due to the proximity of the water presaturation at 4.75 ppm. All four Gly NH appear as triplets with $J_{NH,H\alpha}$ = 6 Hz. For several resolved doublets in Figure 4, the value of $J_{NH,H\alpha}$ lies in the narrow range of 6.4–6.8 Hz. This and the general uniformity of the $J_{NH,H\alpha}$ splittings seen in the COSY plot (Figure 5) suggest that the peptide backbone undergoes rapid conformational averaging of the ϕ angles with no significant contribution from stable helix (J = ca. 4 Hz) or β-sheet (J = ca. 9 Hz) structures.

For the NOESY experiment in H_2O buffer, strong intraresidue Overhauser effects were observed for Phe and Tyr but no interresidue effects between aromatic side chains. Some weak and apparently nonspecific NOE contacts were observed between Met and Ala methyls and the aromatics. NOEs in the aliphatic region were very weak, consistent with a high degree of segmental motion (NOE nulling). A ROESY experiment, which is not susceptible to nulling effects due to rapid motion, gave the full pattern of intraresidue effects [e.g., Hβ to aromatic H(2,6) correlations for Phe and Tyr assisted in the assignments], and most of the intraresidue NH–Hα correlations were detectable, except for A^{46} and very weak Gly cross-peaks. Approximately 8–10 interresidue Hα to NH cross-peaks ($d_{\alpha N}$ < 5 Å; Wüthrich, 1986) were observed and appear to be sequential effects; e.g., V^{20} Hα to S^{21} NH could

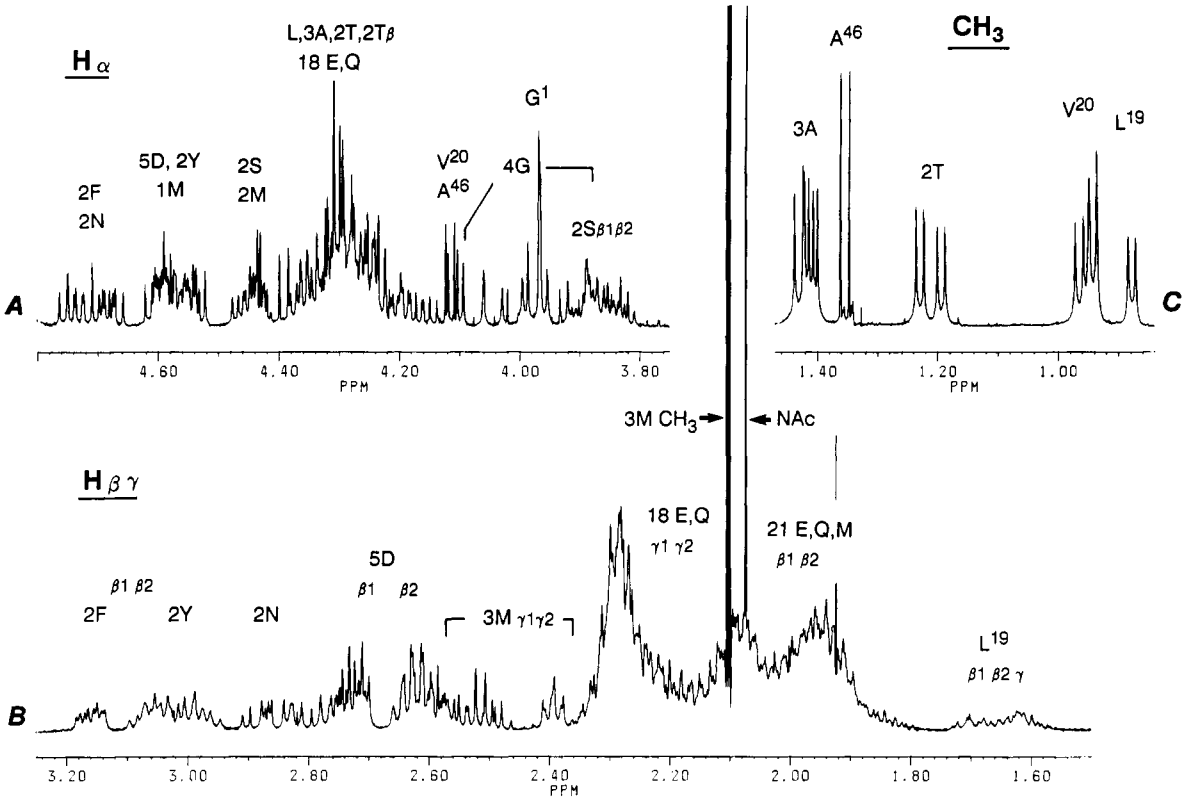

FIGURE 2: 1-D 500-MHz ^{1}H-NMR spectrum (aliphatic proton regions) of the synthetic N^{α}-Ac-β-tubulin(400–445) peptide in PBS/D_2O buffer, pH 6.98, 20 °C (see Experimental Procedures). Assignments of individual spin systems and amino acid types (numbers and one-letter codes) have been made using 2-D techniques. Sequence-specific assignments could be made in only a few cases.

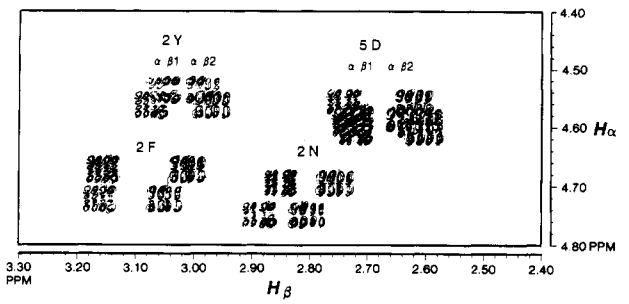

FIGURE 3: Small portion of the 500-MHz 2-D COSY-DQF experiment for the sample of Figure 2. The Hα,Hβ correlation cross-peaks for 11 ABX spin systems are grouped together according to the nature of the amino acid side chain.

be assigned, and G^1 to E^2, E^2 to G^3, and Y^{26} to D^{28} are tentative. Unequivocal assignments are made difficult by the large number of near-degeneracies (14 E, 5 D, etc.). No NH to NH cross-peaks were detected, indicating the absence of helix. In view of the conclusion that the peptide shows little secondary structure, a more detailed analysis of the NMR results was not carried out.

Circular Dichroism. The CD spectrum of the peptide at pH 7.4 corresponds to a secondary structure content of 66% random coil, 30% reverse turn, and <5% helix (Figure 6A). The addition of any amount of β-sheet structure in the calculations only reduced the quality of the fit to the data. The presence of a large excess of Ca^{2+} or Mg^{2+} did not produce any significant change in the spectrum (Figure 6B). At pH 3.0, however, a condition where the charges on the Glu and Asp side chains should be neutralized, the CD spectrum was altered (Figure 6C). The calculated α-helix content rose to about 25%, the remainder being 55–60% random coil and 15–20% reverse turn. In 8 M urea (Figure 6D), a significant change in the spectrum resulted. The ellipticity in the 210–220-nm region, where was negative in phosphate buffer, became distinctly positive in 8 M urea, the rotational strength being almost identical to that of model peptides in a pure random-coil conformation.

When the peptide was exposed to increasing concentrations of trifluoroethanol (TFE) (Figure 7), an increase in α-helix content was observed. The amount of helical content increased linearly with the TFE concentration, reaching 70% helix at 80% TFE. This change was achieved principally at the expense of random coil, with the reverse-turn content remaining relatively constant after an initial small decrease, until it is completely lost at 100% TFE.

It has been proposed that a 50% methanol in water or a 50% ethanol in water solution reproduces to some extent the conditions of solvent polarity existing in the interior of a protein (Tanford, 1962; Nozaki & Tanford, 1971). The tubulin β-peptide in this solution exhibits a CD spectrum (Figure 6C) corresponding to about 30% helix, 50% random coil, and 20% reverse turn, a secondary structure content very similar to that seen at pH 3.0 (but with slightly more helix) and somewhat similar to that seen in 25% TFE.

The nine C-terminal residues of the tubulin β-peptide are especially rich in glutamate residues and constitute one of the two regions in the peptide with the strongest theoretical helix-forming propensity. The potential effect on the secondary structure of eliminating these nine residues was investigated. The truncated peptide in phosphate buffer (Figure 8A) shows little difference in overall conformation, the curve being fitted by 55–60% random coil, 35–40% reverse turn, and <5% helix. Once again, this was not altered in the presence of Ca^{2+} or Mg^{2+} (Figure 8B) or in 100 mM NaF (Figure 8D). Likewise, 8 M NaF had no effect on the spectrum (data not shown). Under those conditions favoring helix formation in the intact β-peptide, however, the truncated peptide did not adopt so

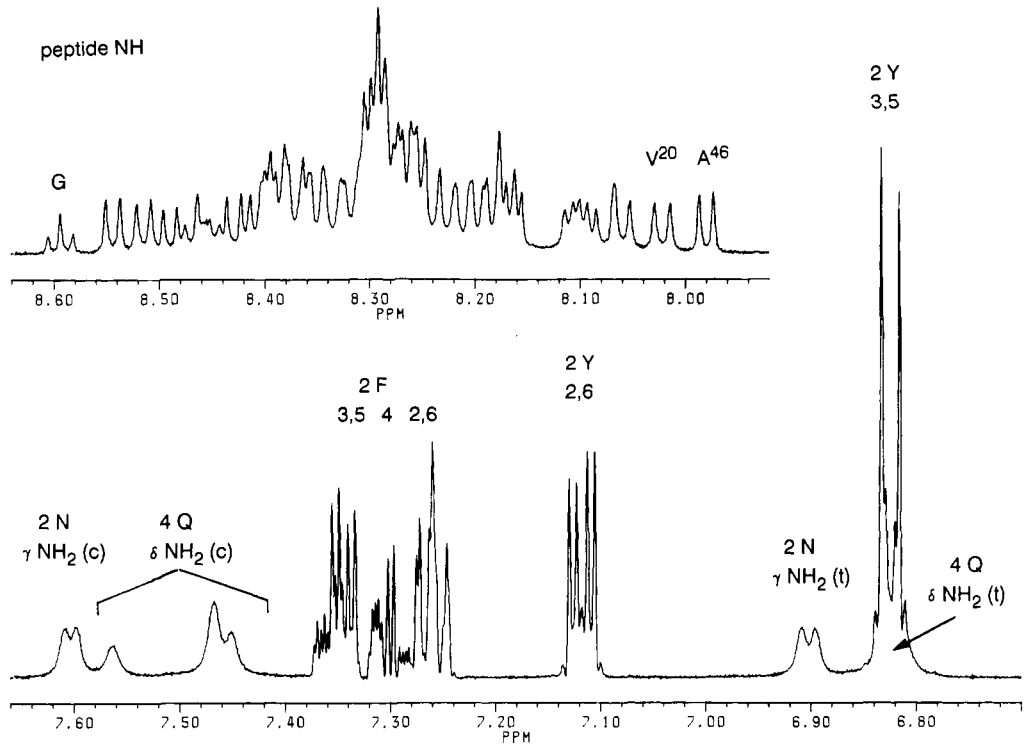

FIGURE 4: Expansion of the low-field portion of the 1-D spectrum obtained for the peptide in PBS/H_2O buffer, pH 5.6, 30 °C. Although water suppression by presaturation was used, at least 40 peptide NH (by integration) are detectable as well as all 12 nonequivalent side-chain amide protons (c = proton cis to carbonyl, t = trans). The aromatic ring protons are numbered with the convention that C1 = Cγ.

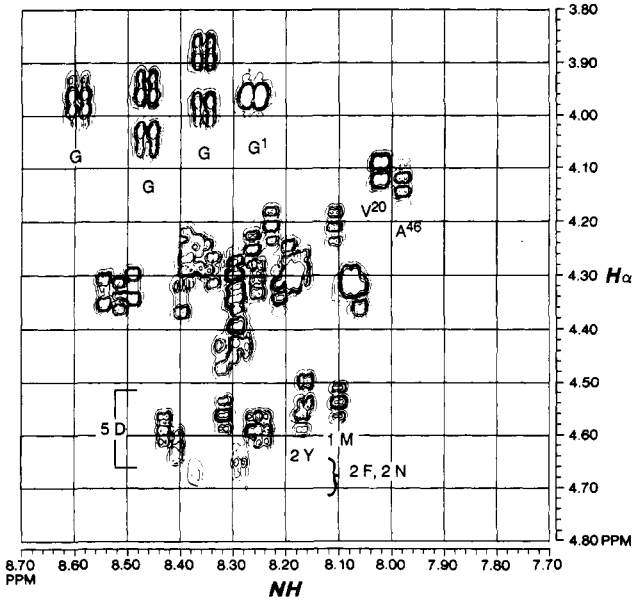

FIGURE 5: Hα,NH correlation region for a magnitude-mode COSY experiment with the sample of Figure 4. A number of assignments could be made directly; the central bulk of signals includes 14 E, 4 Q, 3 A, and 2 T. The correlations for F and N are partially suppressed due to the water irradiation.

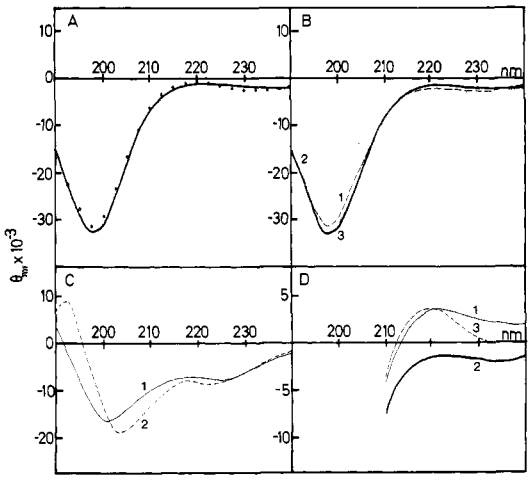

FIGURE 6: Far-UV circular dichroism spectrum of the tubulin β-(400–445) peptide under different solution conditions. The concentration of the peptide was 65 μg/mL. (A) Spectrum in 10 mM sodium phosphate, pH 7.4. Open circles indicate the curve fitted by model peptide spectra. (B) Effect of divalent cations: in 10 mM Tris·HCl, pH 7.4, containing 5 mM $CaCl_2$ (1); in 10 mM sodium phosphate containing 5 mM $MgCl_2$ (2); the spectrum in the absence of the cations (3) is given for comparison. (C) Effect of lowering the pH to 3.0 (2 mM HCl) (1) and of 1:1 CH_3OH/H_2O (2). (D) Effect of denaturation in 8 M urea: tubulin β-peptide in urea (1), in phosphate buffer (2), and model peptide in pure random coil (3).

high a helix content. At pH 3.0 (Figure 8C), the helix moiety is at most 15%, with 57% random coil and 18% reverse turn. Upon titration with TFE, the truncated peptide tends to have less helix, the value at 80% TFE being only 50% α-helix (data not shown).

Tubulin Assembly Inhibition. The two peptides were assayed for their tubulin assembly inhibition activity using a filter assay. The concentrations of the peptide solutions were determined from the absorbance at 275 nm since each peptide contains two tyrosine residues. The results are presented in Table I. Both peptides were inhibitory, but the β(400–445) peptide appeared to be about 4 times more active than the β(400–436) peptide in inhibiting assembly. Neither peptide inhibited assembly of pure tubulin in the presence of 10% DMSO, indicating that the inhibition was due to an interaction with MAPs.

DISCUSSION

The C-terminal regions of the α- and β-tubulin polypeptides play an important role in the self-assembly of tubulin. Removal

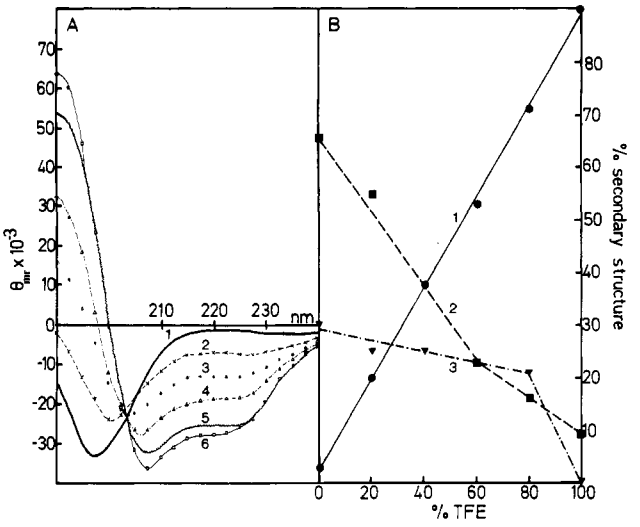

FIGURE 7: TFE titration of tubulin β(400–445) peptide. (A) CD spectra in (1) 0%, (2) 20%, (3) 40%, (4) 60%, (5) 80%, and (6) 100% TFE. (B) Percent secondary structure as a function of TFE concentration: (1) α-helix; (2) random coil; (3) reverse turn.

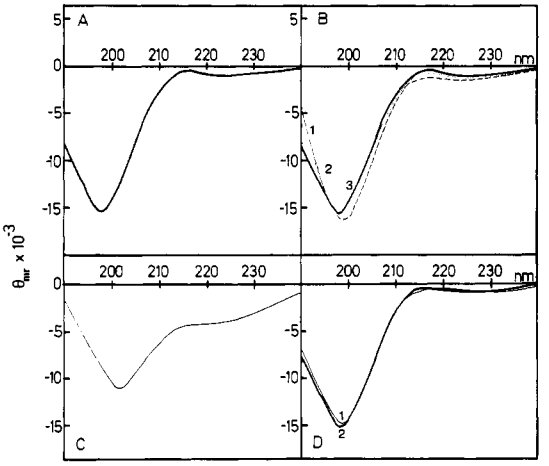

FIGURE 8: Far-UV circular dichroism spectra of the tubulin β(400–436) peptide. The concentration of the peptide was 84 μg/mL. (A) Spectrum in 10 mM sodium phosphate buffer, pH 7.4. (B) Effect of divalent cations. Symbols as in Figure 6B. (C) Spectrum at pH 3.0. (D) Spectrum in 100 mM NaF in phosphate buffer (1) [spectrum in phosphate alone (2) given for comparison].

Table I: Inhibition of Tubulin Assembly by β C-Terminal Peptides[a]

peptide	concn (mM)	tubulin assembled (μM)	% inhibn
β(400–445)	0	8.7	
	0.24	5.7	34
	0.48	2.7	69
β(400–436)	0	8.4	
	0.83	5.2	38
	1.65	1.2	86

[a] Tubulin (10 μM, 1 mg/mL) was incubated with MAPs (0.2 mg/mL), 0.5 mM [^{3}H]GTP, and the peptides in PEM at 37 °C for 10 min as described under Experimental Procedures.

of these regions by proteolysis stimulates the rate of assembly into polymorphic structures (Serrano et al., 1984b, 1988; Sackett et al., 1985; Bhattacharyya et al., 1985; White et al., 1987). Conversion of side-chain carboxyl functions in these regions to neutral amides also stimulates tubulin polymerization, but into microtubules (Mejillano & Himes, 1991). Proteolytic removal of the C-termini or modification of the carboxyl groups also decreases the interaction of tubulin with MAPs. From studies involving binding to MAPs or inhibition of MAP-stimulated assembly, it has been proposed that major sites on tubulin for MAP interaction are in the β(422–440) sequence (Littauer et al., 1986; Maccioni et al., 1988; Cross et al., 1991). Peptides encompassing the βII(422–434) and βII(434–440) sequences showed the best activity in inhibiting MAP-stimulated tubulin polymerization, while a peptide containing the βI(408–426) sequence was inactive (Cross et al., 1991). The C-terminal β(400–445) peptide we used is equivalent to the βII isotype of mammalian brain tubulin. Cross et al. (1991) found that the βII(434–440) peptide was about 20% less effective in inhibiting tubulin assembly than the βII(422–434) peptide. On the other hand, we found that removal of residues 437–445 diminished the competition of the peptide for MAPs. This apparent discrepancy could result from the comparison of two separate peptides with a single peptide containing the same residues and having more sites of interaction. In other words, a βII(422–440) peptide might have a higher binding affinity than the βII(422–434) peptide. In addition, residues 441–445 may also contribute to the binding energy.

Some studies on the solution conformation of the β(422–434) peptide have been done, primarily in CH_3OH/H_2O mixtures (Otter et al., 1991). Small acyclic peptides often lack much regular secondary structure, and since it is thought that the last 40–45 amino acids in the C-termini are exposed to solvent, we decided to look at the conformation of the entire β(400–445) sequence. This stretch of 46 amino acids contains 19 Asp and Glu residues and no basic residues. We also examined the same peptide lacking the last nine residues, seven of which are Asp and Glu. Secondary structure prediction programs indicate that a peptide containing the last 46 amino acids should have a large content of α-helix with the segments 401–412 and 426–445 having the highest helix potential (Figure 1) (Krauhs et al., 1981). However, CD experiments showed that at pH 7.4 in low or high ionic strength aqueous solutions, the major contributing structure of both peptides was random coil, with α-helix accounting for less than 5% of the total conformation. The presence of some regular structure was indicated by the negative ellipticity in the 210–220-nm region of the spectrum and the fact that the ellipticity in this region became positive in 8 M urea. Under most conditions, this regular structure was due to the presence of about 30% reverse-turn contribution. This is consistent with three or four bends in the peptide. Whether these bends occur stably at distinct sites as indicated in Figure 1 or represent an average over many different conformations has not been determined.

Taken together, all of the NMR results indicate that β-tubulin 400–445 peptide at pH 5.6 or 7 does not possess any significant amount of regular secondary structure, either α-helix or β-sheet. There must be a uniformly high degree of segmental motion throughout the peptide, e.g., a dynamic equilibrium of random-coil and β-turn structures with extensive averaging of the backbone angles ϕ ($J_{NH,H\alpha}$). Most, if not all, side chains undergo rapid conformational equilibrium ($J_{\alpha\beta}$) with <30% of the rotomers having $\chi^1 = +60°$ ($\alpha\beta1$, $\alpha\beta2$ gauche, gauche). This is completely consistent with the CD results. Although all exchangeable protons are lost to solvent within minutes, the uniformly slow NH exchange rates at pH 5.6 (lifetimes greater than the T_1 relaxation times) may be caused by electrostatic shielding from the 19 negatively charged side chains which hinder the approach of negatively charged hydroxyl or phosphate moieties that can act as base catalysts. NMR studies at low pH were not carried out because the peptide precipitated at the ca. 5 mM concentrations used.

Maccioni et al. (1986) found that subtilisin digestion of tubulin, which cleaves near the C-termini of α- and β-tubulin, produced a peptide fraction with a molecular mass of about 4 kDa and which showed no organized structure as judged by CD. Although this fraction undoubtedly contained a mixture of peptides, the results are consistent with ours.

The C-terminal regions of tubulin contain a high-affinity binding site for Ca^{2+} (Serrano et al., 1986) observed under low ionic strength conditions, and it has been suggested that this region is the site of weak binding by Mg^{2+} (Correia et al., 1988), the result of which could stimulate the assembly reaction. We found that a 400-fold molar excess of Mg^{2+} or Ca^{2+} over the peptide (a 22-fold molar excess over total carboxyl groups) had no effect on the structure of the peptide as detected by CD. However, if one calculates the extent of complexation of cations under these conditions using the stability constant of Mg^{2+} and Ca^{2+} for binding to acetic and propionic acid of 3.2 M^{-1} (O'Sullivan, 1969), it is apparent that only about 2% of the carboxyl groups would be complexed to the cation. Since the concentrations of the cations used influence tubulin assembly (stimulation in the case of Mg^{2+} and inhibition in the case of Ca^{2+}), it is probable that the mechanism of complexation is more intricate, probably involving two or more protein ligands acting in a chelating fashion. In fact, Frigon and Timasheff (1975) determined the K_a for weak binding of Mg^{2+} to multiple sites on tubulin to be 106 M^{-1}, indicating that the binding is indeed more complex than monodentate binding to carboxyl groups.

The absence of significant α-helical structure at neutral pH, in spite of secondary structure predictions, is probably due to repulsive forces between the multiple negative charges, similar to the situation for polyglutamate (Adler et al., 1968). Evidence to support this proposal was the finding with CD that the helical content did rise to 25% at pH 3.0, conditions under which the carboxyls should be protonated. Removal of the highly concentrated region of negative charges represented by the last nine amino acid residues had little effect on the conformation of the peptide at pH 7.4. However, the conformation that the 400–436 peptide assumed at pH 3.0 did not contain as much α-helix as that of the 400–445 peptide, indicating that the last nine residues contribute to the helical content of the total peptide under conditions that promote helix formation. The fact that the ability to inhibit MAP-stimulated assembly of pure tubulin correlates in these two peptides with the amount of α-helix potentially formed suggests that adoption of this structure upon complexation with MAPs may play a role in microtubule assembly. On the other hand, the additional negative charges in the longer peptide may explain its greater inhibitory activity.

The organic solvent TFE had a large effect on the secondary structure, forcing both peptides into a conformation containing increased content of α-helix at the expense of random coil. This effect is thought to be due to the lower hydrogen-bonding capability of TFE relative to H_2O, promoting the formation of internal H-bonds in the peptide. This effect must be strong enough to overcome the repulsive effects of the negative charges. Another possible effect of TFE is to increase the pK_a values of the many carboxyl groups in the peptides under study (Reichardt, 1988), causing them to be protonated. The peptides also showed increased helical content in 50% CH_3OH/H_2O. In an NMR study of the structure of the β(422–434) peptide in 90% CD_3OH/10% H_2O, it was concluded that there is one complete helical turn running from Thr-429 to Gln-433 (Otter et al., 1991). The change in conformation at pH 3.0 and in TFE or CH_3OH could well reflect the ability of this region of β-tubulin to undergo structural changes upon binding to MAPs or other ligands. Such interactions, by masking the negatively charged carboxyl groups, could produce similar conformational alterations.

The peptides used in this study are found in the βII-tubulin isotype, the major β isotype in mammalian brain (Little & Seehaus, 1988). The C-terminal regions of α- and β-tubulin are subjected to posttranslational modifications: detyrosinylation/tyrosinylation at the C-terminus of α-tubulin (Barra et al., 1973), loss of the terminal Glu-Tyr residues from the α-subunit (Paturle-Lafanechère et al., 1991), polyglutamylation of the α- and β-subunits (Eddé et al., 1990; Alexander et al., 1991; Redeker et al., 1991; Rudiger et al., 1992), and phosphorylation of βIII-tubulin (Alexander et al., 1991). Such modifications could conceivably alter the conformation of these peptides and have ramifications on divalent cation binding.

ACKNOWLEDGMENT

We thank Jürgen Kretschmer and Jeanne Ellermeier for their excellent technical assistance and Dr. Gernot Maier for peptide sequence determinations.

REFERENCES

Adler, A. J., Hoving, R., Potter, J. J., Wells, M., & Fasman, G. D. (1968) *J. Am. Chem. Soc. 90*, 4736–4738.

Alexander, J. E., Hunt, D. F., Lee, M. K., Shabanowitz, J., Michel, H., Berlin, S. C., MacDonald, T. L., Sundberg, R. J., Rebhun, L. I., & Frankfurter, A. (1991) *Proc. Natl. Acad. Sci. U.S.A. 88*, 4685–4689.

Algaier, J., & Himes, R. H. (1988) *Biochim. Biophys. Acta 954*, 235–243.

Bax, A., & Davis, D. G. (1985) *J. Magn. Reson. 63*, 207–213.

Bhattacharyya, B., Sackett, D. L., & Wolff, J. (1985) *J. Biol. Chem. 260*, 10208–10216.

Breitling, F., & Little, M. (1986) *J. Mol. Biol. 189*, 367–370.

Chou, P. Y., & Fasman, G. D. (1978) *Annu. Rev. Biochem. 47*, 251–276.

Chrisma, M., Fasman, G. D., Balaram, H., & Balaram, P. (1984) *Int. J. Pept. Protein Res. 23*, 411–419.

Correia, J. J., Beth, A. H., & Williams, R. C., Jr. (1988) *J. Biol. Chem. 263*, 10681–10686.

Cross, D., Dominguez, J., Maccioni, R. B., & Avila, J. (1991) *Biochemistry 30*, 4362–4366.

Drubin, D., & Kirschner, M. (1986) *Methods Enzymol. 134*, 156–160.

Eddé, B., Rossier, J., Le Caer, J.-P., Desbruyéres, E., Gros, F., & Denoulet, P. (1990) *Science 247*, 74–77.

Frigon, R. P., & Timasheff, S. N. (1975) *Biochemistry 14*, 4567–4573.

Himes, R. H., Burton, P. R., & Gaito, J. M. (1977) *J. Biol. Chem. 252*, 6222–6228.

Hull, W. E. (1987) *Methods Stereochem. Anal. 9*, 67–231.

Kanazawa, K., & Timasheff, S. N. (1989) *J. Protein Chem. 8*, 131–147.

Kessler, H., Griesinger, C., Kerssebaum, R., Wagner, K., & Ernst, R. R. (1987) *J. Am. Chem. Soc. 109*, 607–609.

Krauhs, E., Little, M., Kempf, T., Hofer-Warbinek, R., Ade, W., & Ponstingl, H. (1981) *Proc. Natl. Acad. Sci. U.S.A. 78*, 4156–4160.

Littauer, U. Z., Giveon, D., Thierauf, M., Ginzburg, I., & Ponstingl, H. (1986) *Proc. Natl. Acad. Sci. U.S.A. 83*, 7162–7166.

Little, M., & Seehaus, T. (1988) *Comp. Biochem. Physiol. 90B*, 655–670.

Maccioni, R. B., & Seeds, N. W. (1978) *Arch. Biochem. Biophys. 185*, 262–271.

Maccioni, R. B., Serrano, L., Avila, J., & Cann, J. R. (1986) *Eur. J. Biochem. 156*, 375–381.

Maccioni, R. B., Rivas, C. I., & Vera, J. C. (1988) *EMBO J. 7*, 1957–1963.

Mejillano, M. R., & Himes, R. H. (1991) *J. Biol. Chem. 266*, 657–664.

Nozaki, Y., & Tanford, C. (1971) *J. Biol. Chem. 246*, 2211–2217.

O'Sullivan, W. J. (1986) in *Data for Biochemical Research* (Dawson, R. M. C., Elliott, D. C., Elliott, W. H., & Jones, K. M., Eds.) p 411, Clarendon Press, Oxford.

Otter, A., & Kotovych, G. (1988) *Can. J. Chem. 66*, 1814–1820.

Otter, A., Scott, P. G., Maccioni, R. B., & Kotovych, G. (1991) *Biopolymers 31*, 449–458.

Paturle-Lafanechére, L., Eddé, B., Denoulet, P., Van Dorsselaer, A., Magarquil, H., Le Caer, J. P., Wehland, J., & Job, D. (1991) *Biochemistry 30*, 10523–10528.

Rance, M., Sørensen, O. W., Bodenhausen, G., Wagner, G., Ernst, R. R., & Wüthrich, K. (1983) *Biochem. Biophys. Res. Commun. 117*, 479–485.

Redecker, V., Le Caer, J.-P., Rossier, J., & Promé, J.-C. (1991) *J. Biol. Chem. 266*, 23461–23466.

Reed, J., Hull, W. E., von der Lieth, C. W., Kübler, D., Suhai, S., & Kinzel, V. (1988) *Eur. J. Biochem. 178*, 141–154.

Reichardt, C. (1988) in *Solvents and Solvent Effects in Organic Chemistry*, pp 81–85, VCH, Weinheim, FRG.

Rivas, C. I., Vera, J. C., & Maccioni, R. B. (1988) *Proc. Natl. Acad. Sci. U.S.A. 85*, 6092–6096.

Rudiger, M., Plessman, U., Kloppel, K. B., Wehland, J., & Weber, K. (1992) *FEBS Lett. 308*, 101–105.

Sackett, D. L., Bhattacharyya, B., & Wolff, J. (1985) *J. Biol. Chem. 260*, 43–45.

Serrano, L., Avila, J., & Maccioni, R. B. (1984a) *Biochemistry 23*, 4675–4681.

Serrano, L., de la Torre, J., Maccioni, R. B., & Avila, J. (1984b) *Proc. Natl. Acad. Sci. U.S.A. 81*, 5989–5993.

Serrano, L., Montejo de Garcini, E., Hernández, M. A., & Avila, J. (1985) *Eur. J. Biochem. 153*, 595–600.

Serrano, L., Valencia, A., Caballero, R., & Avila, J. (1986) *J. Biol. Chem. 261*, 7076–7081.

Serrano, L., Wandosell, F., de la Torre, J., & Avila, J. (1988) *Biochem. J. 252*, 683–691.

Shelanski, M. L., Gaskin, F., & Cantor, C. R. (1973) *Proc. Natl. Acad. Sci. U.S.A. 70*, 765–768.

Sober, H. A. (1968) in *CRC Handbook of Biochemistry*, pp 13–18, The Chemical Rubber Co., Cleveland, OH.

Stewart, R. J., Farrell, K. W., & Wilson, L. (1990) *Biochemistry 29*, 6489–6498.

Sugiura, M., Maccioni, R. B., Cann, J. R., York, E. I., Stewart, J. M., & Kotovych, G. (1987) *J. Biomol. Struct. Dyn. 4*, 1105–1107.

Tanford, C. (1962) *J. Am. Chem. Soc. 84*, 4240–4248.

Vera, J. C., Rivas, C. I., & Maccioni, R. B. (1988) *Proc. Natl. Acad. Sci. U.S.A. 85*, 6763–6767.

Vera, J. C., Rivas, C. I., & Maccioni, R. B. (1989) *Biochemistry 28*, 333–339.

Wagner, G. (1983) *J. Magn. Reson. 55*, 151–156.

White, E. A., Burton, P. R., & Himes, R. H. (1987) *Cell Motil. Cytoskeleton 7*, 31–38.

Wilson, L., Snyder, K. B., Thompson, W. C., & Margolis, R. L. (1982) *Methods Cell Biol. 24*, 145–148.

Wüthrich, K. (1986) *NMR of Proteins and Nucleic Acids*, pp 14–19, J. Wiley & Sons, New York.